JACC: CARDIOVASCULAR IMAGING
VOL. 5, NO. 3, SUPPL S, 2012

ISSN 1936-878X/$36.00
PUBLISHED BY ELSEVIER INC.
DOI:10.1016/j.jcmg.2011.11.019

INTRACORONARY IMAGING: LESION CHARACTERISTICS

Definitions and Methodology for the Grayscale and Radiofrequency Intravascular Ultrasound and Coronary Angiographic Analyses

Akiko Maehara, MD,* Ecaterina Cristea, MD,* Gary S. Mintz, MD,* Alexandra J. Lansky, MD,† Ovidiu Dressler, MD,* Sinan Biro, MSc,* Barry Templin, MBA,‡ Renu Virmani, MD,§ Bernard de Bruyne, MD, PhD,‖ Patrick W. Serruys, MD, PhD,¶ Gregg W. Stone, MD*

New York, New York; New Haven, Connecticut; Santa Clara, California; Gaithersburg, Maryland; Aalst, Belgium; and Rotterdam, the Netherlands

OBJECTIVES In a prospective study of the natural history of coronary atherosclerosis using angiography and grayscale and radiofrequency intravascular ultrasound (IVUS)–virtual histology (VH), larger plaque burden, smaller luminal area, and plaque composition thin-cap fibroatheroma emerged as independent predictors of future adverse cardiovascular events.

BACKGROUND The methodology for IVUS-VH classification for an in vivo natural history study and the prospective image mapping by angiography and grayscale and IVUS-VH have not been established.

METHODS All culprit and nonculprit lesions (defined as ≥30% angiographic visual diameter stenoses) were analyzed. Three epicardial vessels as well as all ≥1.5-mm-diameter side branches were divided into 29 CASS (Coronary Artery Surgery Study) segments. Each CASS segment was then subdivided into 1.5-mm-long subsegments, and dimensions were analyzed. All grayscale and IVUS-VH slices from the proximal 6 to 8 cm of the 3 coronary arteries were analyzed, with lesions defined as having more than 3 consecutive slices with ≥40% plaque burden categorized as: 1) VH thin-cap fibroatheroma; 2) thick-cap fibroatheroma; 3) pathological intimal thickening; 4) fibrotic plaque; or 5) fibrocalcific plaque. The locations of angiographic and grayscale and IVUS-VH lesions were recorded in relation to the corresponding coronary artery ostium and nearby side branches.

RESULTS The 3-year cumulative rate of major adverse cardiovascular events was 20.4%. Events were adjudicated to culprit lesions in 12.9% of patients and to nonculprit lesions in 11.6%. On multivariate analysis, nonculprit lesions associated with recurrent events were characterized by a plaque burden ≥70% (hazard ratio: 5.03; 95% confidence interval: 2.51 to 10.11; $p < 0.0001$), a minimal luminal area ≤4.0 mm^2 (hazard ratio: 3.21; 95% confidence interval: 1.61 to 6.42; $p = 0.001$), and IVUS-VH phenotype of a thin-cap fibroatheroma (hazard ratio: 3.35; 95% confidence interval: 1.77 to 6.36; $p < 0.001$).

CONCLUSIONS Three-vessel multimodality coronary artery imaging was feasible and allowed the identification of lesion-level predictors for future events in this natural history study. (J Am Coll Cardiol Img 2012;5:S1–9) © 2012 by the American College of Cardiology Foundation

From the *Columbia University Medical Center and the Cardiovascular Research Foundation, New York, New York; †Yale University School of Medicine, New Haven, Connecticut; ‡Abbott Vascular, Santa Clara, California; §CVPath Institute, Gaithersburg, Maryland; ‖Cardiovascular Center, OLV Hospital, Aalst, Belgium; and the ¶Thoraxcenter/Erasmus University, Rotterdam, the Netherlands. Drs. Maehara and Mintz have received research and grant support from Volcano Corporation and Boston Scientific Corporation. Dr. Mintz is a consultant for Volcano Corporation. Mr. Templin is an employee of Abbott Vascular. Dr. Virmani is a member of the advisory boards of Abbott Vascular, Arsenal Medical, Atrium, Lutonix, Medtronic, and W. L. Gore. Dr. Stone is a consultant for Boston Scientific, Abbott Vascular, Medtronic, The Medicines Company, Volcano Corporation, and InfraReDx. All other authors have reported that they have no relationships relevant to the contents of this paper to disclose.

Manuscript received August 16, 2011; revised manuscript received November 1, 2011, accepted November 3, 2011.

The PROSPECT (Providing Regional Observations to Study Predictors of Events in the Coronary Tree) study was a prospective trial of the natural history of coronary atherosclerosis using angiography and radiofrequency intravascular ultrasound (IVUS)–virtual histology (VH) to identify the clinical and lesion-related factors that predict future coronary events (1). It was performed at 37 sites in the United States and Europe. Patients with acute coronary syndromes

See page S39

were enrolled after undergoing successful percutaneous coronary intervention (PCI) of all culprit lesions responsible for the acute events. Angiography was performed of the entire coronary tree, followed by grayscale and IVUS-VH of the proximal 6 to 8 cm of all 3 epicardial arteries. All baseline angiograms and grayscale and IVUS-VH images were prospectively analyzed without knowledge of subsequent events using prespecified definitions and methodology. Plaque burden and luminal area as prospectively measured by grayscale IVUS and plaque composition as assessed by IVUS-VH were determined to be independent predictors of future adverse cardiovascular events (1).

The main results of the PROSPECT study were as follows. The 3-year cumulative rate of major adverse cardiovascular events was 20.4%. Events were adjudicated to culprit lesions in 12.9% of patients and to nonculprit lesions in 11.6%. On multivariate analysis, nonculprit lesions associated with recurrent events were characterized by a plaque burden ≥70% (hazard ratio: 5.03; 95% confidence interval: 2.51 to 10.11; $p < 0.0001$), a minimal luminal area ≤ 4.0 mm^2 (hazard ratio: 3.21; 95% confidence interval: 1.61 to 6.42; $p = 0.001$), and IVUS-VH phenotype of a thin-cap fibroatheroma (TCFA) (hazard ratio: 3.35; 95% confidence interval: 1.77 to 6.36; $p < 0.001$).

The purpose of this report is to provide detailed information about the methodology used in PROSPECT that arrived at these findings. All reports presented in this issue of *iJACC* (2–9) used uniform methodology and classification as outlined in this report.

ABBREVIATIONS AND ACRONYMS

CSA = cross-sectional area
DC = dense calcium
EEM = external elastic membrane
IVUS = intravascular ultrasound
NC = necrotic core
PCI = percutaneous coronary intervention
PIT = pathological intimal thickening
TCFA = thin-cap fibroatheroma
ThCFA = thick-cap fibroatheroma
TIMI = Thrombolysis In Myocardial Infarction
VH = virtual histology

METHODS

Coronary angiography. Coronary angiography before PCI, immediately after PCI, and at follow-up (at the time of the event) were performed in at least 2 orthogonal views after the administration of intracoronary nitroglycerin.

3-vessel qualitative and quantitative angiographic analysis. All angiograms were analyzed prospectively at an independent angiographic core laboratory at the Cardiovascular Research Foundation (CRF) (New York, New York) that was blinded to the IVUS analysis and to the clinical events. Quantitative analysis was performed using proprietary methodology modified from Medis CMS software version 7.0 (Medis Medical Imaging Systems, Leiden, the Netherlands) that was first validated in 78 randomly selected coronary segments (data on file at the CRF). Qualitative analysis using standard definitions (10) included thrombus, ulceration, intimal flap, aneurysm, tortuosity, angulation, calcification, and eccentricity. Post-PCI qualitative analyses included abrupt closure, ectasia, luminal irregularities, intimal flap, thrombus, dissection, perforation, side branch loss, distal embolization, and coronary spasm. The longitudinal extension of each of these morphologies was recorded in relation to the distance from the coronary ostium. For each vessel, Thrombolysis In Myocardial Infarction (TIMI) flow, TIMI frame count, corrected TIMI frame count, and myocardial blush score were recorded before PCI, after PCI, and at follow-up.

First, all culprit and nonculprit lesions (defined as ≥30% visual diameter stenosis) were identified and their locations recorded in relation to the corresponding coronary artery ostium and nearby side branches.

Second, all culprit and nonculprit lesions before PCI, culprit lesions after PCI, and lesions causing events during follow-up were analyzed, including minimal luminal diameter, lesion length, mean reference vessel diameter (obtained by averaging 5-mm segments proximal and distal to the target lesion location), and diameter stenosis ([1 − minimal luminal diameter/reference vessel diameter] × 100).

Third, all 3 epicardial vessels as well as all ≥1.5-mm-diameter side branches were divided into 29 CASS (Coronary Artery Surgery Study) segments. Each CASS segment was then subdivided into 1.5-mm-long subsegments (Fig. 1) and analyzed. Measurements of each 1.5-mm-long subsegment included minimal luminal diameter, interpolated reference vessel diameter, and diameter stenosis.

Grayscale and IVUS-VH image acquisition. Immediately after PCI, grayscale and IVUS-VH were performed within the left main coronary artery and

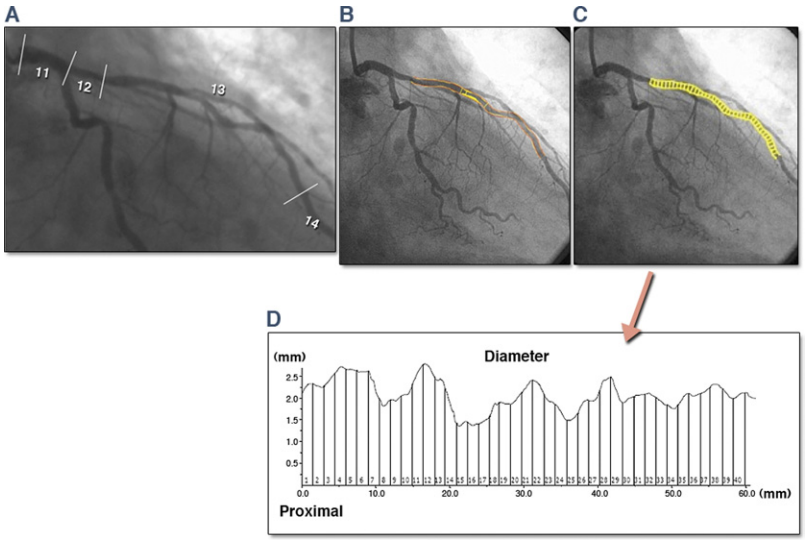

Figure 1. Example of Angiographic Analysis

(A) Left main and left anterior descending coronary artery CASS (Coronary Artery Surgery Study) segments (CASS 11 to 14). **(B)** Typical quantitative analysis of segment 13 and its mid lesion. **(C)** Quantitative angiographic analysis developed for PROSPECT (Providing Regional Observations to Study Predictors of Events in the Coronary Tree); segment 13 was divided into 1.5-mm-long subsegments. **(D)** Output of the angiographic analysis of PROSPECT. The x-axis shows the distance from the proximal to the distal end of this segment and its 1.5-mm-long subsegments. The y-axis shows the luminal diameter for each subsegment.

proximal 6 to 8 cm of each major epicardial coronary artery using a synthetic aperture array, 20-MHz, 3.2-F catheter (Eagle Eye, Volcano Corporation, Rancho Cordova, California) after the administration of intracoronary nitroglycerin. The IVUS catheter was advanced distal to the region of interest, the guiding catheter was disengaged, and the IVUS catheter was pulled backed to the aorto-ostial junction using an R-100 motorized catheter pullback system (0.5 mm/s). During pullback, grayscale IVUS images were recorded, raw radiofrequency data were captured at the top of the R wave, and the reconstruction of the color-coded map by an IVUS-VH data recorder was performed (In-Vision Gold, Volcano Corporation). IVUS studies were archived onto CD-ROMs or DVDs.

Grayscale and IVUS-VH analysis. Off-line grayscale and IVUS-VH analyses of all imaged segments were performed prospectively at an independent IVUS core laboratory at the CRF that was blinded to the angiographic analysis and to the clinical events using: 1) QCU-CMS software (Medis Medical Imaging Systems) for contouring; 2) pcVH version 2.1 software (Volcano Corporation) for contouring and data output; and 3) proprietary qVH software (developed and validated at the CRF) for qualitative segmental assessment and quantitative data output. External elastic membrane (EEM) and luminal borders were contoured for each slice (median interslice distance 0.40 mm). Quantitative IVUS measurements included EEM cross-sectional area (CSA), luminal CSA, plaque and media (EEM minus luminal) CSA, and plaque burden (plaque and media divided by EEM). IVUS-VH plaque components were color coded as dense calcium (DC) (white), necrotic core (NC) (red), fibrofatty (light green), or fibrous tissue (dark green) and reported as CSA and percents of total plaque CSA (11–13). Volumes were calculated using Simpson's rule and reported as total volume and normalized area (volume divided by length). The slice with the minimal luminal CSA and the slice with maximal NC CSA were identified and assessed as well. The remodeling index was calculated by the EEM CSA at the minimal luminal CSA or maximal NC slice divided by the average of the proximal and distal reference EEM CSA. Qualitative grayscale IVUS morphology included plaque rupture (intraplaque cavity that communicated with the lumen with an overlying residual fibrous cap fragment) and echolucent plaque (a plaque containing a non–echo-reflective dark zone). Because the left main coronary artery was usually imaged during both left anterior descending and left circumflex coronary artery pullbacks, the run with better left main image quality was chosen. Similarly, when a proximal vessel was imaged during pullbacks from both the distal main vessel and a major side branch,

the run with better proximal vessel image quality was chosen.

IVUS-VH classification. IVUS-VH phenotype was classified as: 1) VH TCFA; 2) thick-cap fibroatheroma (ThCFA); 3) pathological intimal thickening (PIT); 4) fibrotic plaque; and 5) fibrocalcific plaque. Fibrotic plaque had mainly fibrous tissue, with <10% confluent NC, <10% confluent DC, and <15% fibrofatty plaque. Fibrocalcific plaque had mainly fibrous tissue, with >10% confluent DC but <10% confluent NC. PIT had a mixture of all plaque components but predominantly fibrofatty plaque, with <10% confluent NC and <10% confluent DC (Fig. 2).

Fibroatheroma (both VH TCFA and ThCFA) was defined as >10% confluent NC (spotty red color was not considered confluent NC) (Fig. 3). Because the resolution of IVUS-VH is 150 to 250 μm, it was not possible to detect fibrous cap thickness <65 μm (the typical pathologic definition of a thin fibrous cap). Therefore, if there was >30° of NC abutting to the lumen in three consecutive slices, the fibroatheroma was classified as VH TCFA; otherwise, it was classified as ThCFA. IVUS-VH often contains a 1-pixel thickness of white separating the NC from the luminal surface that is considered to be an artifact; this was included in the qualitative assessment of NC. The total NC abutting the lumen including the isolated nonred pixels was measured in degrees (Fig. 3).

Fibroatheromas were subclassified as having single or multiple confluent NCs (circumferential or layered) and containing or not containing DC (Fig. 2). Because DC caused shadowing and may have affected IVUS-VH plaque classification, we reported DC in relation to the NC: DC superficial to NC, DC inside of NC, or DC outside of NC. For this purpose, grayscale IVUS was evaluated together with IVUS-VH to assess the presence and extent of shadowing from calcification.

Thus, all individual image slices were evaluated regarding: 1) existence of fibroatheroma (>10% confluent NC); 2) existence of a fibrous cap; 3) single or multiple NCs (layered or circumferential); and 4) presence of DC and its relation with NC (superficial to NC, inside of NC, or outside of NC). An overall hierarchy of fibroatheroma subtypes was pre-specified as follows (on the basis of their anticipated likelihood to be correlated with future adverse events):

1. VH TCFA, multiple confluent NC, DC outside of NC
2. VH TCFA, multiple confluent NC, no DC
3. VH TCFA, single confluent NC, DC outside of NC

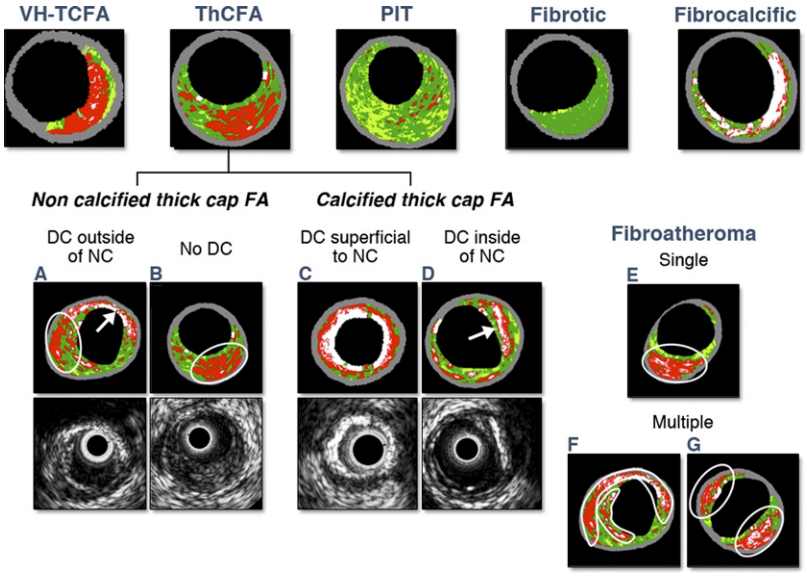

Figure 2. IVUS-VH Phenotype Classification

Typical intravascular ultrasound (IVUS)–virtual histology (VH) examples of VH thin-cap fibroatheroma (TCFA), thick-cap fibroatheroma (ThCFA), pathological intimal thickening (PIT), fibrotic plaque, and fibrocalcific plaque. ThCFA was subdivided into necrotic core (NC) outside of dense calcium (DC) **(A)** or no DC **(B)** and DC superficial to NC **(C)** or DC inside of NC **(D)**, respectively. Fibroatheroma (FA) was subdivided into single FA **(E)** or multiple FA (layered multiple **[F]** or circumferential multiple **[G]**).

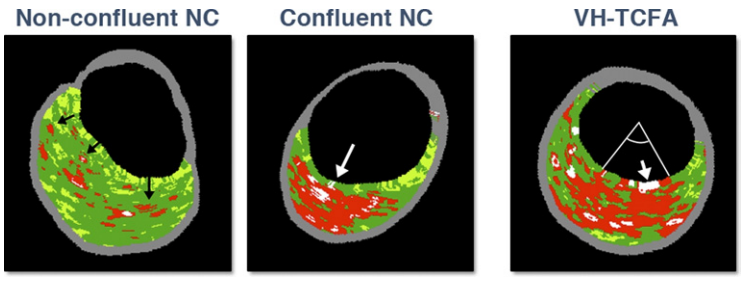

Figure 3. Nonconfluent and Confluent NC and VH TCFA

Nonconfluent necrotic core (NC) typically appeared as spotty red color **(black arrows)** in the plaque. Confluent NC had a thick and continuous red color **(white arrow)**. A typical virtual histology (VH) thin-cap fibroatheroma (TCFA) included an arc of abutting NC to the lumen of 50° (angle); this NC contained an occasional white or other nonred pixel within the abutting NC **(white arrow)**.

4. VH TCFA, single confluent NC, no DC
5. ThCFA, multiple confluent NC, DC outside of NC
6. ThCFA, multiple confluent NC, no DC
7. ThCFA, single confluent NC, DC outside of NC
8. ThCFA, single confluent NC, no DC
9. ThCFA, multiple confluent NC, DC superficial to NC or inside of NC
10. ThCFA, single confluent NC, DC superficial to NC or inside of NC

These 10 fibroatheroma subtypes were divided into 3 main groups 1) VH TCFA (subtypes 1 to 4), 2) noncalcified ThCFA (subtypes 5 to 8), and 3) calcified ThCFA (subtypes 9 and 10).

Lesion-level and fibroatheroma-level analysis. In addition to vessel data and overall patient data, we constructed the grayscale and IVUS-VH data at 3 levels: lesion level, fibroatheroma level, and slice level (Fig. 4). A lesion was defined as a segment in which ≥3 consecutive slices had ≥40% plaque burden. Lesions were considered separate if there was a ≥5-mm-long normal segment with <40% plaque burden between them. For lesion level IVUS-VH classification, the entire lesion was evaluated.

A lesion could contain more than 1 fibroatheroma. The main fibroatheroma groups (VH TCFA, noncalcified ThCFA, and calcified ThCFA) required 3 consecutive slices demonstrating the same main fibroatheroma subtype. Fibroatheromas were considered multiple and distinct if they were separated by ≥3 consecutive image slices containing a different fibroatheroma subtype (VH TCFA, noncalcified ThCFA, or calcified ThCFA) or nonfibroatheroma phenotype; for example, multiple VH TCFAs were considered separate if they were separated by ≥3 consecutive non–VH TCFA–containing image slices. Then, the fibroatheroma subtype (1 to 10 as specified previously) was assigned on the basis of the maximum NC slice. Grayscale morphology (plaque rupture and echolucent plaque) was also mapped at the fibroatheroma level.

In lesions with more than 1 fibroatheroma subtype, for the lesion level VH classification, the previously described hierarchy was used; a VH TCFA took precedence over a ThCFA, and any

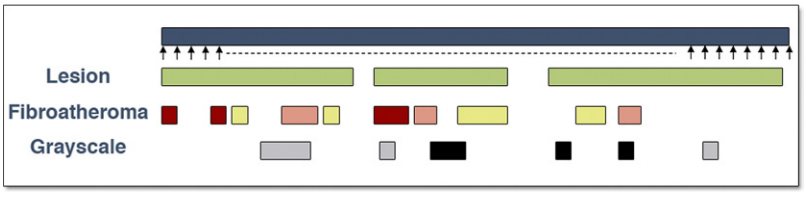

Figure 4. Three Levels of Grayscale and IVUS-VH

The **arrows** associated with the **blue line** indicate consecutive intravascular ultrasound (IVUS) image slices within a vessel segment; each slice contains unique IVUS data. The **3 green lines** indicate that this segment contains 3 lesions. The **yellow, red, and orange lines** indicate that each lesion contains more than 1 nonoverlapping fibroatheroma: virtual histology (VH) thin-cap fibroatheroma **(yellow)**, noncalcified-cap fibroatheroma **(red)**, or calcified-cap fibroatheroma **(orange)**, respectively. Grayscale morphology (shown in **gray or black**) such as plaque rupture or echolucent plaque was also mapped to the overall segment **(blue line)**, to individual lesions **(green lines)**, and to the fibroatheromas **(yellow, red, or orange lines)**.

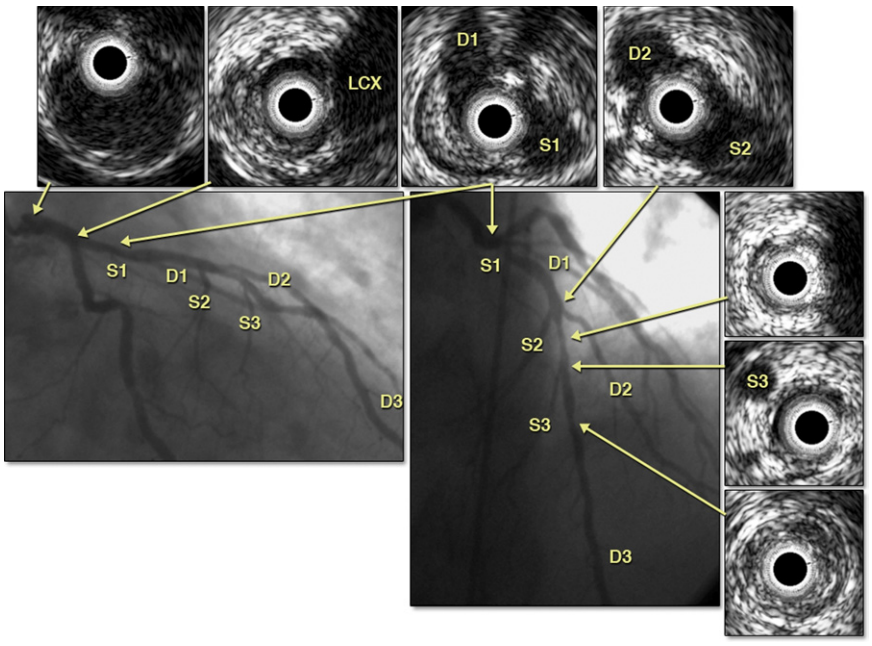

Figure 5. Coregistration Between Angiography and IVUS

Angiographic and intravascular ultrasound (IVUS) segments were matched using side branches as fiduciary landmarks. D1 = first diagonal branch; D2 = second diagonal branch; LCX = left circumflex coronary artery; S1 = first septal perforator; S2 = second septal perforator; S3 = third septal perforator.

fibroatheroma took precedence over any nonfibroatheroma. If there was no fibroatheroma in the entire lesion, the VH classification at the minimal luminal area site was evaluated and defined as fibrotic plaque, fibrocalcific plaque, or PIT.

Coregistration with IVUS-VH and identification of lesions responsible for nonculprit events. All angiographic and grayscale and IVUS-VH analyses were performed independently. Grayscale and IVUS-VH analyses of all imaged epicardial vessels were coregistered to the angiographic roadmap using fiduciary side branches for alignment (Fig. 5) with interpolation as necessary to account for different length measurements to define and match the 1.5-mm-long angiographic and grayscale and IVUS-VH slices and subsegments. Lesions responsible for events were identified using the follow-up angiogram, and then the corresponding segments and subsegments were matched side by side to the baseline angiograms and their corresponding baseline grayscale and IVUS-VH images in terms of both quantitative and qualitative morphologic analysis (Fig. 6).

DISCUSSION

Development of definitions. Previous angiographic natural history studies, such as CASS, demonstrated that patients with normal coronary arteries have a relatively benign prognosis. Like PROSPECT, CASS defined normal coronary arteries as having <30% diameter stenosis by visual estimation (14,15). Glagov et al. (16) described the concept of "compensated remodeling" and concluded that compensation by vessel enlargement failed and luminal encroachment began when plaque accumulation (i.e., plaque burden) exceeded (on average) 40% of EEM area. Many plaque regression and progression studies have reported an average overall plaque burden in the study segments of approximately 40% (17,18). Many IVUS substudies of interventional trials have reported an average reference segment plaque burden of 40% (19). Again, this justifies the use of a plaque burden of 40% as the minimal threshold to define a lesion.

The minimal reported length of a pathologic TCFA is 1 to 2 mm (20–22). Antegrade or retrograde movement of an IVUS catheter during the systolic and diastolic cycle averages 1.5 mm (23). In past studies, the average interslice distance in the electrocardiographically gated VH images was 0.5 mm. For these reasons, PROSPECT used a 1.5-mm (or 3 image slice) minimal length for any finding such as plaque burden ≥40%, VH TCFA, and so on.

The IVUS-VH phenotype classification is based on the modified American Heart Association classification, excluding adaptive intimal thickening, intimal xanthoma, and fatty streaks, because these are typically present only in arteries with <40% plaque burden (20). In addition, the next most common high-risk lesion morphology, plaque erosion, cannot be reliably detected by IVUS, because of its limited resolution. Therefore, for IVUS-VH classification, only the following phenotypes were considered: 1) TCFA; 2) ThCFA; 3) PIT; 4) fibrotic plaque; and 5) fibrocalcific plaque. Pathologically, the key difference between PIT and fibroatheroma is the presence of an NC. Therefore, to define fibroatheroma, we chose the presence of confluent NC ≥10% because Virmani et al. (20,21) and Cheruvu et al. (22) reported that the amounts of overall NC for TCFA, ThCFA, and stable plaque were 23 ± 17%, 15 ± 20%, and 12 ± 25%.

IVUS-VH–related issues. The accuracy of IVUS-VH analysis behind calcium continues to be debated and probably depends on the thickness, density, and amount of calcium. However, it is unclear how often there is a definable signal compared with mostly noise behind calcium from images obtained in vivo. In cases with grayscale shadowing, VH often shows red color, which is in fact an artifact. We did not exclude data behind grayscale calcification, which may have introduced errors.

There is currently no specific VH algorithm to identify thrombus (11–13). Thus, thrombus appears green or light green (fibrotic or fibrofatty plaque) depending on its age. In the VH analysis in PROSPECT, no attempt was made to identify thrombus and to exclude it from the overall plaque area. Therefore, thrombus could cause a TCFA to be misclassified as a ThCFA.

Data acquisition issues. As previously reported, of 697 enrolled patients, grayscale and IVUS-VH images were available for 673 and 623 patients, respectively (1). Grayscale IVUS images were not available in 24 patients, because: 1) the core lab never received any IVUS image media (n = 17); 2) there was too much noise in the IVUS images (n = 4); 3) pullback length was inadequate (n = 2); and 4) there were problems with the digital media (n = 1). IVUS-VH images were not available for 50 patients, because of: 1) failure to capture IVUS-VH

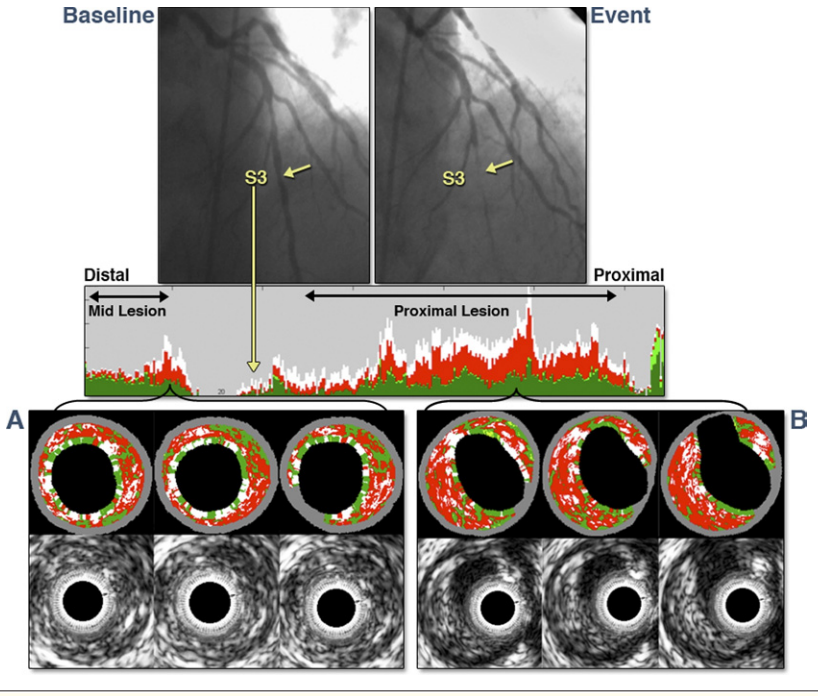

Figure 6. Example of a Lesion With a Nonculprit MACE

At baseline, a 58-year-old man presented with a non–ST-segment elevation myocardial infarction, and the culprit lesion in the right coronary artery was treated. All 3 vessels were imaged, and the angiograms and intravascular ultrasound (IVUS)–virtual histology (VH) images for the left anterior descending coronary artery at baseline are shown. One year later, the patient was rehospitalized for unstable angina, with coronary angiography showing total occlusion of the mid left anterior descending coronary artery (S3 on the angiogram). The corresponding baseline IVUS-VH images for the lesion causing the nonculprit major adverse cardiac event (MACE) (mid lesion, IVUS-VH image **A**) showed a thin-cap fibroatheroma with a minimal luminal cross-sectional area of 3.6 mm^2.

data (n = 28, in whom only grayscale IVUS was received); 2) too much noise (n = 6), segmental loss of VH (n = 4), or other catheter-related problems (n = 3); and 3) digital media–related problems (n = 9). Eleven patients (1.6%) had complications that were attributed to 3-vessel intravascular imaging. Mostly, these complications occurred in the early stages of the trial during the learning curve.

Both the angiographic and IVUS-VH analyses were time consuming. Even when performed by experienced analysts and overread by experienced physicians, the angiographic analysis for the entire coronary tree required at least 1 day per patient, and the grayscale and IVUS-VH analysis required on average 1 day per vessel (mean 2.3 days per patient). Thus, given the software that was available at the time of this study, the total manpower required for the complete PROSPECT analysis was estimated to be 2,400 person-days. In addition, because the development of IVUS-VH algorithm and analysis software continued during the trial, several reanalyses were performed. The size of the entire image set for 697 patients was 1.5 terabytes (2.1 gigabytes/patient). During the analysis process to protect the data, multiple image files were kept on an active server with regular backup; this required approximately 6 terabytes of storage space.

Comparison with other technologies and future directions. There are 2 other radiofrequency IVUS analytic techniques available: iMAP (Boston Scientific Corporation, Natick, Massachusetts) and integrated backscatter IVUS. Each of the 3 IVUS tissue characterization techniques uses a different algorithm, tissue color coding, and analysis scheme, and there is no uniform methodology or standard for reporting the results of IVUS-derived plaque composition, making direct comparisons difficult. In addition, there are also structural and compositional optical imaging techniques (optical coherence tomography and near infrared spectroscopy); in particular, the resolution of optical coherence tomography will allow direct measurement of vulnerable plaque fibrous cap thickness, something that was not possible in PROSPECT. There are enough differences among these diverse intravascular imaging modalities to make it difficult to use the findings of PROSPECT for any technology other than IVUS-VH (24–28); each technology will probably require its own PROSPECT-like study. Furthermore, even another natural history study using IVUS-VH should be performed only after a reevaluation the image acquisition and analysis methodology and definitions used in PROSPECT.

Conversely, the systematic approach to integrating angiography, intravascular imaging, and clinical follow-up as performed in PROSPECT should be useful guidelines for any future study.

CONCLUSIONS

PROSPECT was a natural history study in patients with acute coronary syndromes in which 3-vessel angiography and grayscale and radiofrequency IVUS were used to prospectively characterize 3,160 IVUS lesions and to identify the patient-related and lesion-related predictors of events. Accomplishing this required the development of proprietary software to permit coregistration of angiographic and IVUS images and detailed analysis at a level not previously attempted. Future software iterations should allow these processes to be automated and streamlined, reducing their complexity and personnel burden, thereby facilitating future natural history studies and drug and device therapy trials.

Reprint requests and correspondence: Dr. Akiko Maehara, Cardiovascular Research Foundation, 111 East 59th Street, New York, New York 10022. *E-mail: amaehara@crf.org.*

REFERENCES

1. Stone GW, Maehara A, Lansky AJ, et al. A prospective natural history study of coronary atherosclerosis. N Engl J Med 2011;364:226–35.
2. Wykrzkowska JJ, Mintz GS, Garcia-Garcia HM, et al. Longitudinal distribution of plaque burden and necrotic core–rich plaques in nonculprit lesions of patients presenting with acute coronary syndromes. J Am Coll Cardiol Img 2012;5 Suppl S:S10–8.
3. Brugaletta S, Garcia-Garcia HM, Serruys PM, et al. Relationship between palpography and virtual histology in patients with acute coronary syndromes. J Am Coll Cardiol Img 2012;5 Suppl S:S19–27.
4. Marso SP, Mercado N, Maehara A, et al. Plaque composition and clinical outcomes in acute coronary syndrome patients with metabolic syndrome or diabetes. J Am Coll Cardiol Img 2012;5 Suppl S:S42–52.
5. Baber U, Stone GW, Weisz G, et al. Coronary plaque composition, morphology, and outcomes in patients with and without chronic kidney disease presenting with acute coronary syndromes. J Am Coll Cardiol Img 2012;5 Suppl S:S53–61.
6. Lansky AJ, Ng VG, Maehara A, et al. Gender and the extent of coronary atherosclerosis, plaque composition and clinical outcomes in acute coronary syndromes. J Am Coll Cardiol Img 2012;5 Suppl S:S62–72.
7. McPherson JA, Maehara A, Weisz G, et al. Residual plaque burden in patients with acute coronary syndromes after successful percutaneous coronary intervention. J Am Coll Cardiol Img 2012;5 Suppl S:S76–85.

8. Brener SJ, Mintz GS, Cristea E, et al. Characteristics and clinical significance of nonculprit, angiographically mild lesions in acute coronary syndromes. J Am Coll Cardiol Img 2012;5 Suppl S:S86–94.
9. Sanidas EA, Mintz GS, Maehara A, et al. Adverse cardiovascular events arising from atherosclerotic lesions with and without angiographic disease progression. J Am Coll Cardiol Img 2012;5 Suppl S:S95–105.
10. Popma JJ, Almonacid A, Lansky AJ. Qualitative and quantitative coronary angiography. In: Topol EJ, editor. Textbook of Interventional Cardiology. Philadelphia, PA: Saunders, 2008:1071–93.
11. Nair A, Kuban B, Tuzcu M, et al. Coronary plaque classification with intravascular ultrasound radiofrequency data analysis. Circulation 2002;106:2200–6.
12. Nair A, Margolis P, Kuban B, et al. Automated coronary plaque characterization with intravascular ultrasound backscatter: ex vivo validation. Eurointervention 2007;3:113–20.
13. García-García HM, Mintz GS, Lerman A, et al. Tissue characterization using intravascular radiofrequency data analysis: recommendations for acquisition, analysis, interpretation and reporting. Eurointervention 2009; 5:177–89.
14. Ellis S, Alderman E, Cain K, et al. Prediction of risk of anterior myocardial infarction by lesion severity and measurement method of stenoses in the left anterior descending coronary distribution: a CASS registry study. J Am Coll Cardiol 1988;11:908–16.
15. Kemp HG, Kronmal RA, Vlietstra RE, et al. Seven year survival of patients with normal or near normal coronary arteriograms: a CASS registry study. J Am Coll Cardiol 1986;7: 479–83.
16. Glagov S. Weisenberg E, Zarins CK, et al. Compensatory enlargement of human atherosclerotic coronary arteries. N Eng J Med 1987;316:1371–5.
17. Nissen ES, Tuzcu EM, Schoenhagen P, et al. Effect of intensive compared with moderate lipid-lowering therapy on progression of coronary atherosclerosis. JAMA 2004;291:1071–80.
18. Nissen ES, Tradif JC, Nicholls SJ, et al. Effect of torcetrapib on the progression of coronary atherosclerosis. N Eng J Med 2007;356:1304–16.
19. Mintz GS, Painter JA, Pichard AD, et al. Atherosclerosis in angiographically "normal" coronary artery reference segments: an intravascular ultrasound study with clinical correlations. J Am Coll Cardiol 1995;25: 1479–85.
20. Virmani R, Kolodgie FD, Burke AP, Farb A, Schwartz SM. Lessons from sudden coronary death. A comprehensive morphological classification scheme for atherosclerotic lesions. Arterioscler Thromb Vasc Biol 2000;20: 1262–75.
21. Virmani R, Bruke AP, Farb A, Kolodgie FD. Pathology of the vulnerable plaque. J Am Coll Cardiol 2006;47:C13–8.
22. Cheruvu PK, Finn AV, Gardner C, et al. Frequency and distribution of thin-cap fibrotatheroma and ruptured plaques in human coronary arteries. J Am Coll Cardiol 2007;50:940–9.
23. Arbab-Zadeh A, DeMaria AN, Penny WF, et al. Axial movement of the intravascular ultrasound probe during the cardiac cycle: implications for three-dimensional reconstruction and measurements of coronary dimensions. Am Heart J 1999; 138:865–72.
24. Sawada T, Shite J, Garcia-Garcia HM, et al. Feasibility of combined use of intravascular ultrasound radiofrequency data analysis and optical coherence tomography for detecting thin-cap fibroatheroma. Eur Heart J 2008;29:1136–46.
25. Goderie TP, van Soest G, Garcia-Garcia HM, et al. Combined optical coherence tomography and intravascular ultrasound radio frequency data analysis for plaque characterization. Classification accuracy of human coronary plaques in vitro. Int J Cardiovasc Imaging 2010;26:843–50.
26. Kubo T, Nakamura N, Matsuo Y, et al. Virtual histology intravascular ultrasound compared with optical coherence tomography for identification of thin-cap fibroatheroma. Int Heart J 2011;52:175–9.
27. Okubo M, Kawasaki M, Ishihara Y, et al. Tissue characterization of coronary plaques: comparison of integrated backscatter intravascular ultrasound with virtual histology intravascular ultrasound. Circ J 2008;72:1631–9.
28. Shin ES, Garcia-Garcia HM, Ligthart JM, et al. In vivo findings of tissue characteristics using iMap IVUS and virtual histology IVUS. Eurointervention 2011;6:1017–9.

Key Words: acute coronary syndromes ■ coronary angiography ■ intravascular ultrasound